Atomic Clocks in Satellite Gravimetry
Investigation of Precision Requirements by Closed Loop Simulations

Moritz Huckfeldt, Florian Wöske and Benny Rievers

This presentation participates in OSPP
Outstanding Student & PhD candidate Presentation contest

Problem Definition

- Satellite velocity not known precisely enough to seperate potential and velocity term (general and special relativity, **Eq.1**)
- Linear Doppler dominates fractional frequency measurement (**Eq.2**)
- 10^{-18} measurement uncertainty reached with nm/s velocity precision

➢ Application of Doppler corrected frequency shifts

Closed Loop Setup

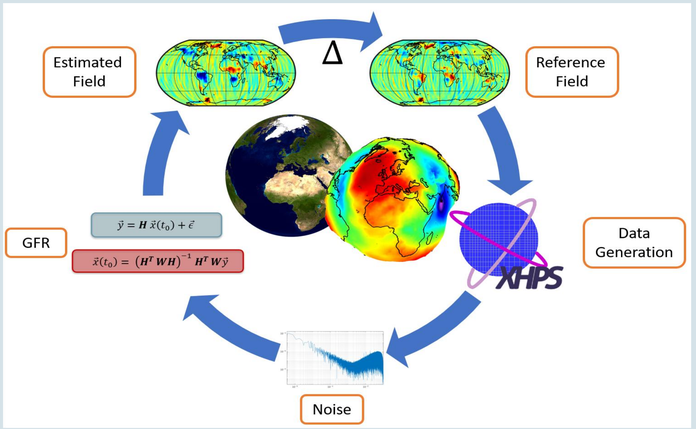

Fig1: Illustration of Closed-Loop GFR Setup

Data Generation

Satellite orbit propagation and environment modeling based on

- Satellite FE model
- Static / *time dependent* SHC
- *Tides, AOD*
- *pN-Corrections*
- *Direct 3rd body acceleration*
- *Direct Sun radiation*
- *Earth albedo and IR radiation*
- *Satellite thermal radiation*
- *Residual atmospheric drag*

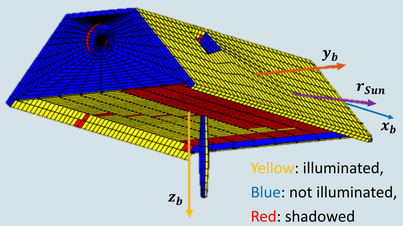

Yellow: illuminated,
Blue: not illuminated,
Red: shadowed

Fig2: Illumination conditions for one direction $\mathbf{r}_{\mathbf{Sun}}$

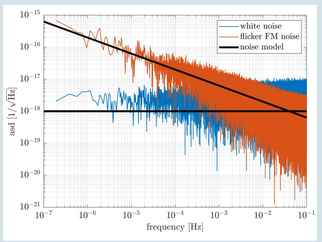

Fig3: Noise models for clock observation

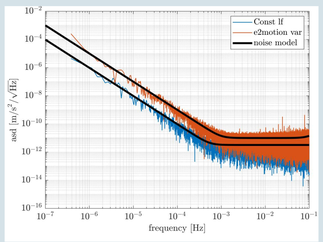

Fig4: Noise models for non-grav. accelerations

Mock Data generation through application of noise models

- Position: white noise σ=2cm
- Acceleration: e2motion var.
- Inter-Satellite Range: realistic KBR
- Clock Observation: white noise σ=10^{-18}

Mock Data Products:

- Position (GNV)
- Attitude (SCA)
- Accelerometer (ACC)
- Inter-Satellite Range/Range-Rate (KBR)
- Clock Observation (QCL)

Estimated Gravity Fields Utilizing Clock Observations

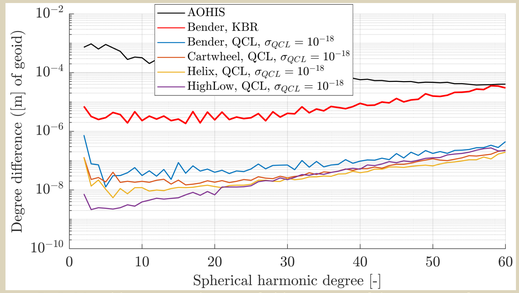

Fig8: Monthly estimated gravity fields in terms of degree error for different satellite scenarios

Scenarios

- Bender formation with realistic KBR measurement as reference
- Significant improvement for clocks with σ=10^{-18}
- Cartwheel and Helix very similar
  - Drifting due to atmospheric drag is limiting estimation precision
  - Crosstrack portion in Helix gives small benefit
- High-Low constellation best for low degrees

Clock Observation Noise

- Assumptions
  - Laser system available with better uncertainty than clocks (realistic technology assumption)
  - Precise pointing possible (Carthwheel and Helix exhibit significantly higher relative velocities)
  - Clock uncertainty reached after 5s (realistic integration times see below)
- Noise can be increased up to σ=10^{-16} to enable improved estimated gravity fields

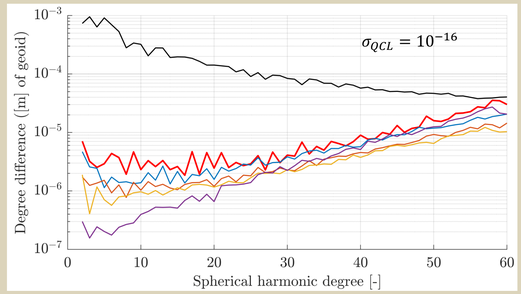

Fig9: Monthly estimated gravity fields in terms of degree error for different satellite scenarios with QCL noise of σ=10^{-16}

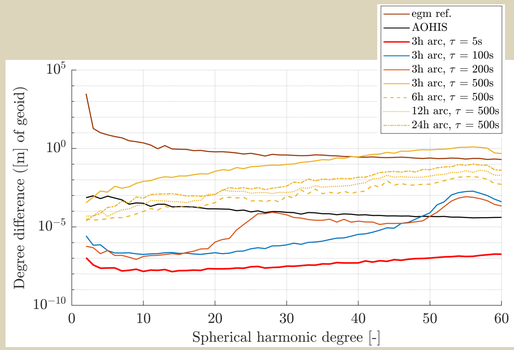

Fig10: Monthly estimated gravity fields in terms of degree error for Helix formation with different clock integration times τ

Clock Integration Time

- Low clock uncertainty is result of statistics
  - Longer integrations time, better frequency knowledge
- Clock integration time cannot be increased arbitrarily in GFR
  - Correlation of time between measurements and resolvable degrees
  - Resonance according to:

$$n = \frac{40000\ km}{v_{sat}\ \tau} = \frac{40000\ km}{7.6 km/s\ 200s} \approx 26$$

- Ill-conditioned problem with low number of observations

Conclusion

- Time-wise GFR approach circumvents velocity precision requirement:
  - Estimation with GNSS and Clock observation instead of independent observation
- Estimation precision: ≈6µm/s
  - Requirement not reached

Linear Doppler vital signal for GFR despite uncertainty

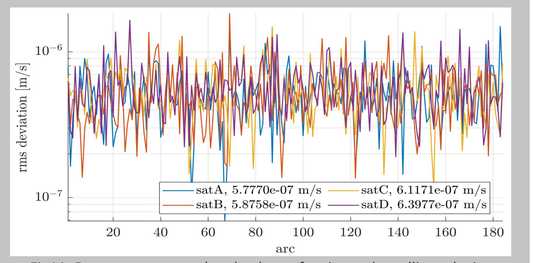

Fig11: Root mean square (rms) values of estimated satellite velocity deviation for each arc in Bender constellation

Clock Observation Models

Frequency comparison between satellites via laser

- Ideal $\frac{\Delta\nu}{\nu_A} = \frac{\Delta U}{c^2} + \frac{\Delta v^2}{2c^2}$ **(Eq.1)**

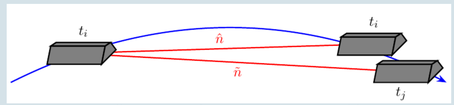

Fig5: Illustration of Emitter-Receiver Problem

- Realistic $\frac{\Delta\nu}{\nu_A} = -\frac{\vec{n}\cdot\Delta\vec{v}}{c} - \frac{(\vec{n}\cdot\vec{v}_A)(\vec{n}\cdot\vec{v}_B)}{c^2} + \frac{(\vec{n}\cdot\vec{v}_B)^2}{c^2} + \frac{\Delta U}{c^2} + \frac{\Delta v^2}{2c^2} - \frac{\Delta U(\vec{n}\cdot\Delta\vec{v})}{c^3} - \frac{(v_A^2 - v_B^2)(\vec{n}\cdot\Delta\vec{v})}{2c^3} - \frac{(\vec{n}\cdot\vec{v}_A)(\vec{n}\cdot\vec{v}_B)^2}{c^3} + \frac{(\vec{n}\cdot\vec{v}_B)^3}{c^3}$ **(Eq.2)**

Realistic clock frequency comparison between satellites include the transmission of a laser signal, which introduces a linear Doppler term into the equation and necessitates the solving of the emitter-receiver problem to determine the correct emission direction.

Satellite Constellations

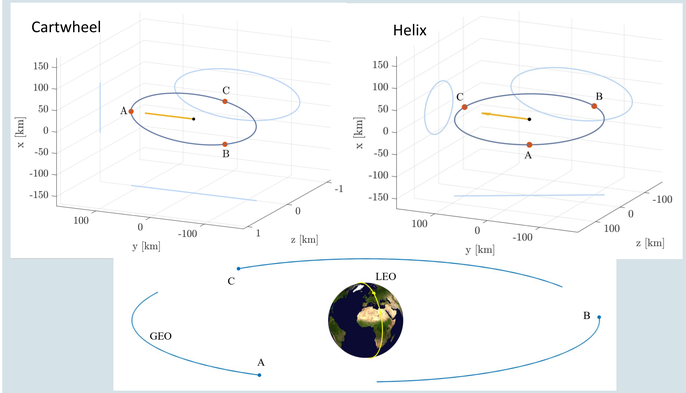

Fig6: Geometry of Cartwheel, Helix and High-Low formation. Yellow arrow describes flight direction.

Time-Wise GFR Approach

Classical variational equations approach

Determination of parameters of a dynamic model to fit the observation data „optimally"

Dynamical model: $m\,\ddot{\vec{X}}_{sat} = \sum \vec{F} = \vec{F}_{Earth} + \vec{F}_{ocean\ tides} + \vec{F}_{solid\ Earth\ tides} + \vec{F}_{atm\ tides} + \vec{F}_{pole\ tides} + \vec{F}_{pN} + \vec{F}_{non-grav.} + \ldots$

Parameters:

Global (for all arcs)	Local (for single arc)
Spherical Harmonic Coefficients C_{nm}, S_{nm}	Initial position of each satellite $\boldsymbol{r_{sat}}$
	Initial velocity of each satellite $\boldsymbol{v_{sat}}$
	Accelerometer calibration parameters ***b, s, d***

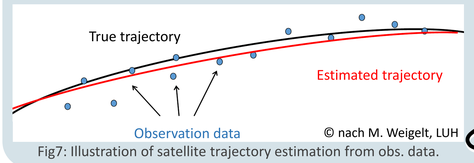

Fig7: Illustration of satellite trajectory estimation from obs. data.

University of Bremen

Acknowledgment

This work was part of the Collaborative Research Center 1464 TerraQ and funded by Deutsche Forschungsgemeinschaft DFG.

DFG Deutsche Forschungsgemeinschaft German Research Foundation

Contact:
moritz.huckfeldt@zarm.uni-bremen.de

CENTER OF APPLIED SPACE TECHNOLOGY AND MICROGRAVITY
ZARM